Supplementary Information

Efficient electrocatalytic ammonia synthesis with FeS_2 coupled MoS_2 heterostructure under ambition conditions

Bo Wang[a], Chao Yan[a], Guangqing Xu[a,b], Xia Shu[a,b], Jun Lv[a,b]*, Jiewu Cui[a,b], Dongbo Yu[a,b], Zhiyong Bao[a,b], Yucheng Wu[a,b]*

a. School of Materials Science and Engineering, Hefei University of Technology, Hefei, 230009, PR China

b. Key Laboratory of Advanced Functional Materials and Devices of Anhui Province, Hefei, 230009, PR China

* Corresponding author. Key Laboratory of Advanced Functional Materials and Devices of Anhui Province, Hefei University of Technology, Hefei, 230009, PR China.

E-mail addresses: lvjun117@126.com (J. Lv), ycwu@hfut.edu.cn (Y. C. Wu).

Experimental

Synthesis of FeS_2/MoS_2

To synthesize the FeS_2/MoS_2 (Fe: Mo= 1: 1) sample, one should follow these steps: Firstly, 241.9 mg of $Na_2MoO_4 \cdot H_2O$, 175.4 mg of $FeCl_3$, 2878 mg of $H_4SiO_4(W_3O_9)_4$, and 450.8 mg of CH_3CSNH_2 were dissolved in 45 mL DI water to prepare the precursor solution, keep stirring the mixture solution to obtain a homogenous solution. Secondly, the solution was transferred into a 60 mL stainless steel autoclave for hydrothermal reaction which was performed at 200 °C for 24 h, and then cool down naturally. Finally, the FeS_2/MoS_2 powders were collected by the centrifugal process, washed with DI water and ethanol several times, then dried for later use. While for the preparation of FeS_2/MoS_2 (Fe: Mo= 1: 2) sample, only the amount of $FeCl_3$ is replaced with 87.7 mg. For FeS_2/MoS_2 (Fe: Mo= 2: 1) sample, only the amount of $FeCl_3$ is replaced with 350.9 mg. For MoS_2 sample, the precursor remains unchanged except that $FeCl_3$ is not included.

Electrochemical measurement

Electrochemical measurements were performed on a CHI660D electrochemical analyzer (Chenhua Instrument, Inc.) in an H-type cell with Nafion 117 membrane. 0.1 M Na_2SO_4 aqueous solution was adopted as the electrolyte. A platinum foil (10mm*10 mm), Ag/AgCl (saturated KCl) and Carbon paper (10mm*10 mm) deposited with electrocatalysts were employed as the counter electrode, the reference electrode and the working electrode, respectively. In this work, the electrode potential (Ag/AgCl) is converted to the reversible hydrogen electrode (RHE) according to the following formula:

$$V\,(\mathrm{RHE}) = V\,(\mathrm{Ag/AgCl}) + 0.197\ \mathrm{V} + 0.059*\mathrm{pH} \quad (1)$$

To well prepare the working electrode, the following steps are suggested: 5 mg of

catalyst, 470 μL of C_3H_8O (IPA) and 30 μL of Nafion solution (5 wt%) were added together. The mixture was suffered from the ultrasound process until a uniform solution was obtained. Then, 10 μL of the slurry was dropped onto the carbon paper (CP) electrode and dried naturally. LSV measurement was recorded from 0 V vs. Ag/AgCl to -1 V vs. Ag/AgCl with a sweep rate of 10 mV/s. EIS measurement was performed at -0.3 V in the range of 0.1–100 kHz.

Determination of NH_3

The general indophenol blue method was employed for the detection of NH_3 concentration[1]. 50 μL of the oxidizing solution containing NaClO (ρCl = 4–4.9) and NaOH (0.75 M), 50 μL of catalyst solution containing 1wt% $Na_2[Fe(CN)_5NO]\cdot_2H_2O$, and 500 μL of coloring solution containing 0.4 M $C_7H_6O_3$ and 0.4 M NaOH solution was added into 4 mL reacted electrolyte in turn. After full-color rendering, the absorbance of electrolytes was recorded at λ = 697 nm. Besides, a series of standard NH_4Cl solutions were used to calibrate the concentration–absorbance curves and the fitting curve is y = 0.243x + 0.054, R^2 = 0.999 (Fig. S5).

NH_3 yield rate is calculated by:

$$NH_3 \text{ yield rate} = (C_{NH4Cl} \times V) / (t \times A) \quad (2)$$

Faradaic efficiency is calculated by:

$$\text{Faradaic efficiency} = (3F \times C_{NH4Cl} \times V) / Q \quad (3)$$

where C_{NH4Cl} is the measured concentration of NH_3, V is the electrolyte volume, t is the potential applied time, A is the surface area of the working electrode, F is the Faraday constant and Q is the quantity of total charge during NRR.

Determination of N_2H_4

The Watt and Chrisp method was employed to detect the possible N_2H_4 in the electrolyte[2]. Firstly, prepare the color reagent: mixing 5.99 g of p-$C_9H_{11}NO$, 30 mL of HCl and 300 mL of C_2H_5OH together. 5 mL color reagent was added into 5 mL reacted electrolyte. After full-color rendering, the absorbance of electrolytes was recorded at λ = 457 nm by spectrophotometer. A series of standard N_2H_4 solutions were used to calibrate the concentration–absorbance curves and the fitting curve is y = 5.654x +

0.0246, R^2 = 0.9997 (Fig. S7).

Determination of NO_3^-

Firstly, 0.1 mL of 1.0 M HCl was added into 5 mL sample solutions. Then, after standing for 5 min, the absorbance of electrolytes was measured by spectrophotometer at a wavelength range from 190 to 300 nm. A series of standard NO_3^- solutions were used to calibrate the concentration–absorbance curves (0.1, 0.2, 0.5, 1.0, 1.5, 2.0, 2.5, 3.0, 4.0 and 5.0 μg mL^{-1} $LiNO_3$ standard solutions) and the fitting curve is y = 0.0571x + 0.0054, R^2 = 0.999, which is recorded with the absorbance value difference at 220 nm and 275 nm as y axis and the concentration of NO_3^- as x axis. (Fig. S8).

Determination of NO_2^-

The Griess-llosvay reaction was employed to detect the possible NO_2^- in the electrolyte. Firstly, prepare the color reagent A and B respectively: Reagent A: 0.5 g of sulfanilamide was dissolved in 50 mL solution consisting of 2.0 M HCl; Reagent B: 50 mg of N-(1-Naphthyl) ethylenediamine dihydrochloride was dissolved in 50 mL of DI water. Secondly, 0.1mL reagent A was added into 5 mL sample solutions, and keep shanking and standing the sample solution for 10 min. Then 0.1 mL of reagent B was added and the mixed solution was shaken up and stand for 30 min. Finally, after full-color rendering, the absorbance of electrolytes was measured by spectrophotometer at a wavelength range from 400 to 700 nm. A series of standard NO_2^- solutions were used to calibrate the concentration–absorbance curves (10, 20, 30, 40, 50, 60, 80 and 100 μg L^{-1}) and the fitting curve is y = 0.0011x + 0.0019, R^2 = 0.9985, which is recorded with the absorbance value difference at 540 nm and 650 nm as y axis and the concentration of NO_2^- as x axis. (Fig. S9).

Characterization

X-ray diffractometer (X'Pert PRO MPD) was employed to characterize the phase structure of samples with Cu Kα radiation (λ = 1.15406 Å). A photoelectron spectrometer (Thermo/ESCALAB250Xi) was adopted to analyze the elemental composition of samples with Al Kα radiation (1486.60 eV) as the excitation source. The morphologies and structure of samples were investigated by SEM (SU8020) and

TEM (JEM-2100F) measurements. UV-visible absorption spectroscopy was measured on a UV 1800 spectrophotometer.

Computational details

Spin-polarized DFT calculations were performed using the Vienna ab initio simulation package (VASP)[3, 4]. The generalized gradient approximation proposed by Perdew, Burke, and Ernzerhof (GGA-PBE) is selected for the exchange-correlation potential[5]. The pseudo-potential was described by the projector-augmented-wave (PAW) method[6]. The geometry optimization is performed until the Hellmann–Feynman force on each atom is smaller than 0.02 eV·Å^{-1}. The energy criterion is set to 10^{-7} eV in iterative solution of the Kohn-Sham equation. A 0.04 2π/Å K-mesh resolution was applied for the geometry optimization. A higher K-mesh resolution was used for the calculation of density of states. A plane-wave kinetic-energy cutoff of 450 eV was applied. GGA+U method was used for the evaluation of DOS. U_{eff}= U −J = 2.5 eV and J=1.0 eV were set for Fe 3d orbitals[7]. The heterojunction was constructed from FeS_2(111) plane and MoS_2(001) surface.

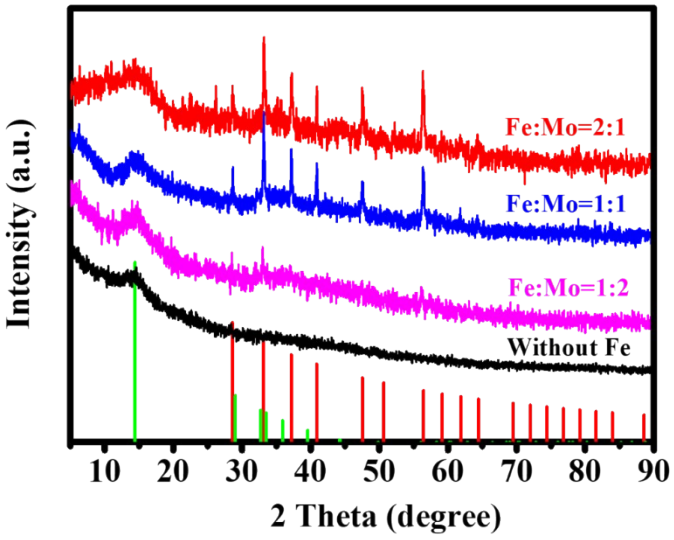

Figure S1. The XRD patterns of FeS_2/MoS_2 powders with different mole ratios (Fe: Mo)

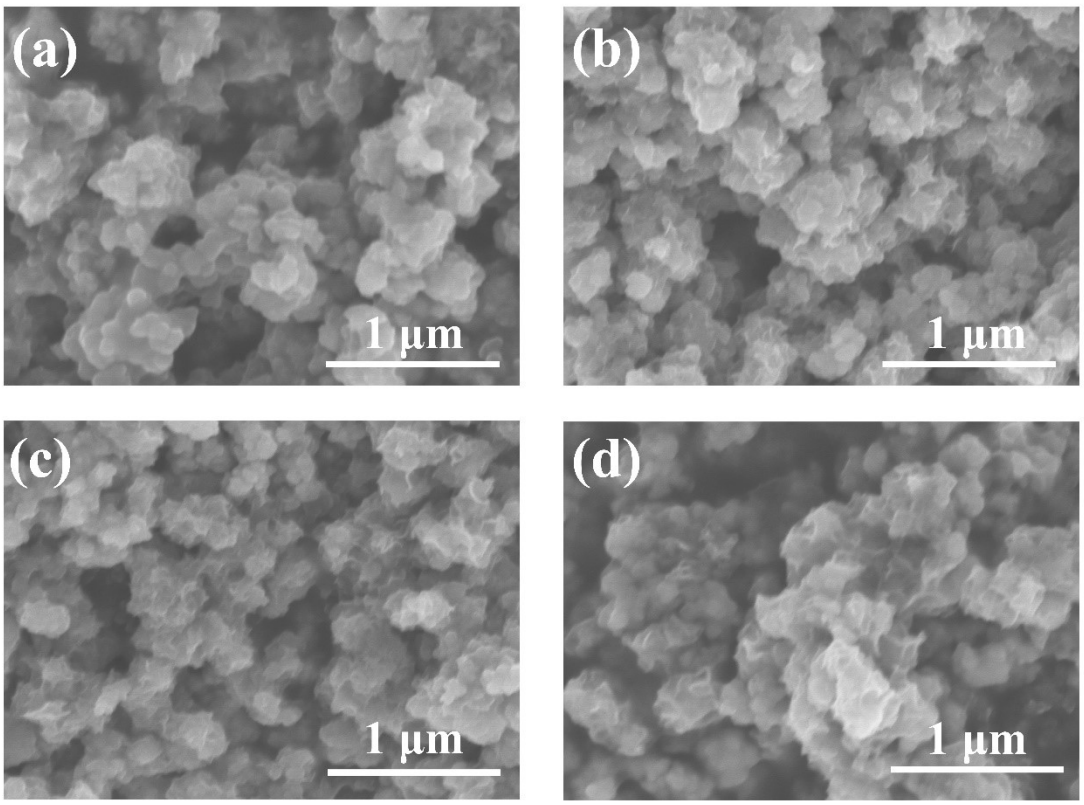

Figure S2. SEM images of different samples, (a) MoS_2, FeS_2/MoS_2 samples (b) Fe: Mo= (1:2), (c) Fe: Mo= (1:1), (d) Fe: Mo= (2:1)

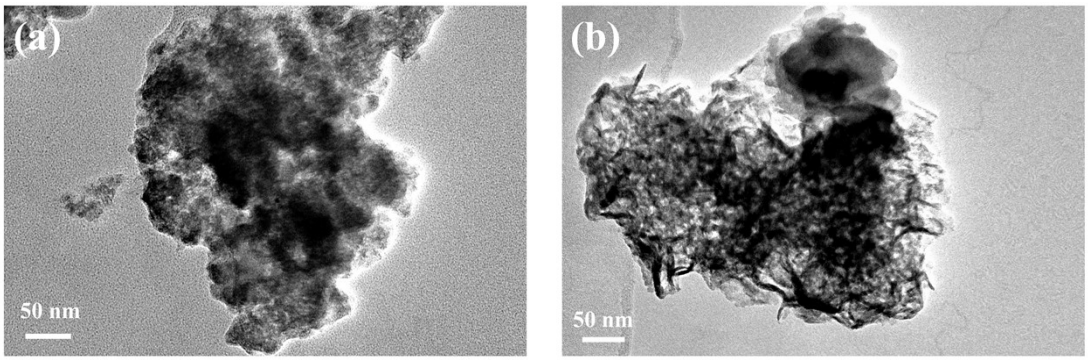

Figure S3. TEM images of different samples, (a) MoS_2, (b)FeS_2/MoS_2(1:1)

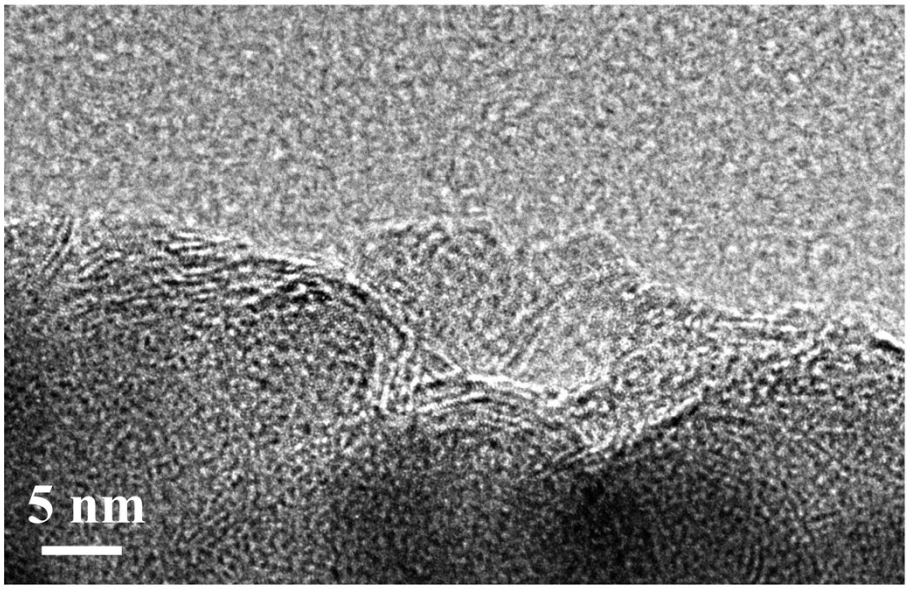

Figure S4. HRTEM image of as-fabricated MoS_2

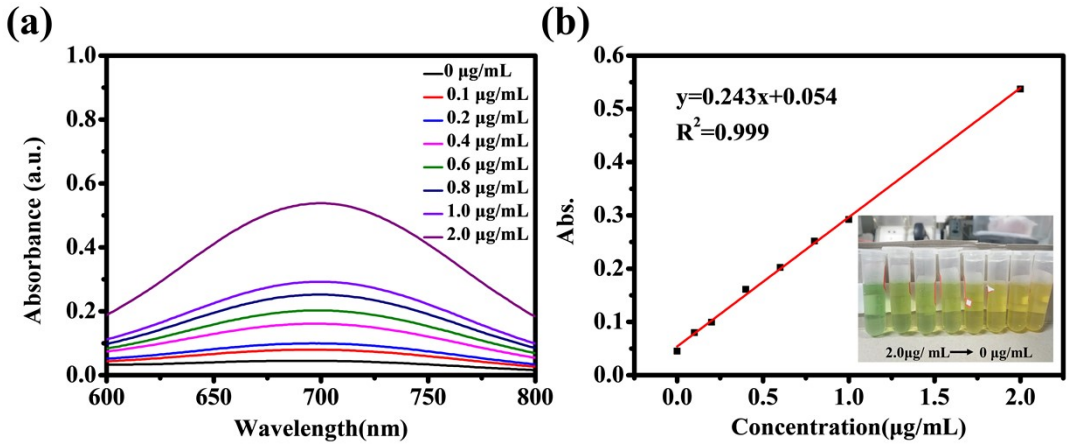

Figure S5. (a) The absorbance of a series of standard solutions for NH_3, (b) the corresponding fitting curve

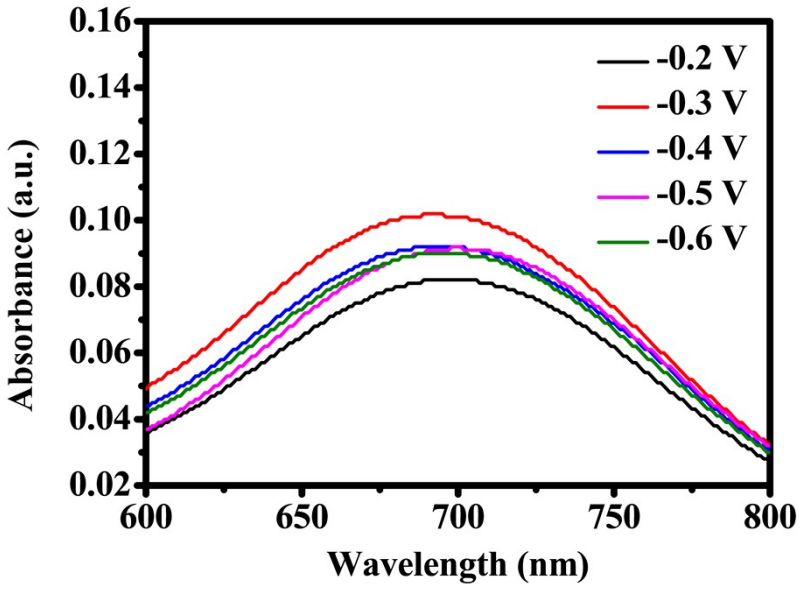

Figure S6. UV−vis absorption spectra of the electrolytes under different potentials

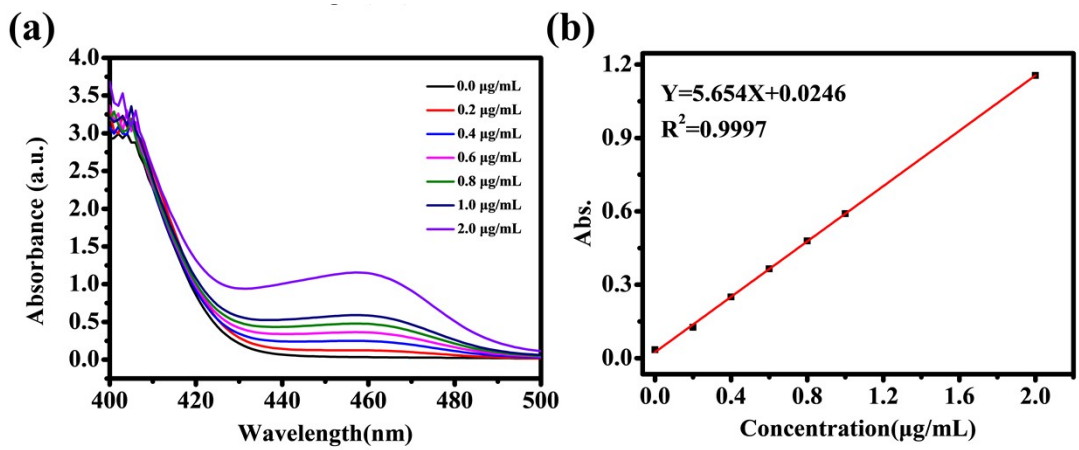

Figure S7. (a) The absorbance of a series of standard solutions for N_2H_4, (b) the corresponding fitting curve

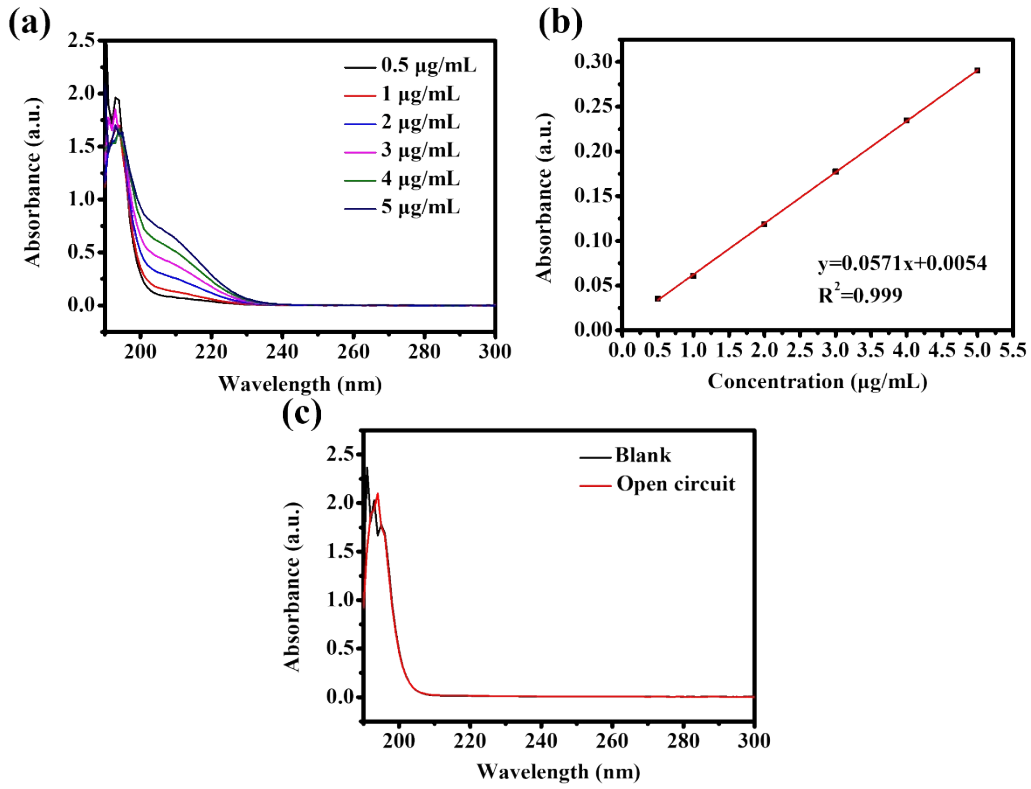

Figure S8. (a) The absorbance of a series of standard solutions for NO_3^-, (b) the corresponding fitting curve, (c) UV−vis absorbance of electrolyte for NO_3^- detection under different conditions

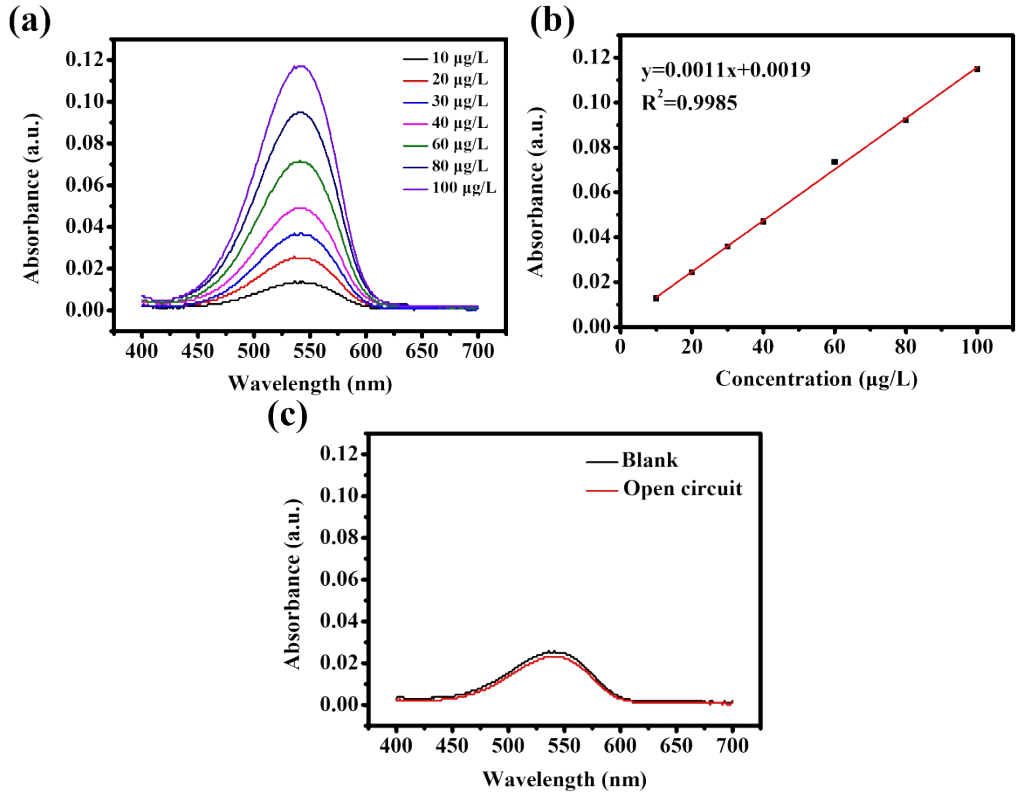

Figure S9. (a) The absorbance of a series of standard solutions for NO_2^-, (b) the corresponding fitting curve, (c) UV−vis absorbance of electrolyte for NO_2^- detection under different conditions

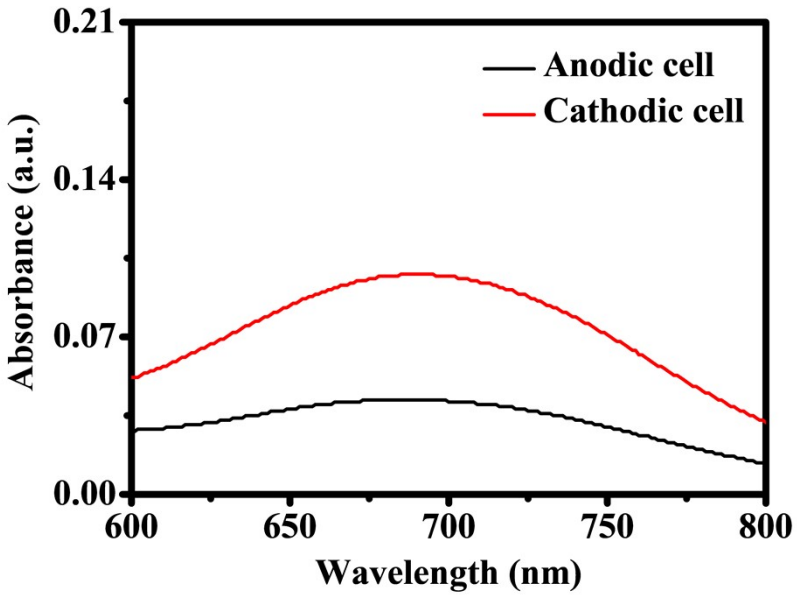

Figure S10. UV−vis absorption spectra of the electrolytes from anodic and cathodic cell

Table S1. The element composition in FeS_2/MoS_2(1:1) sample

Name	Position	At.%
O 1s	532.08	15.38
C 1s	285.08	20.17
S 2p	163.08	45.17
Fe 2p	708.08	1.24
Mo 3d	229.08	18.04

Table S2. The comparison of the NRR performance with the relevant Mo-based catalyst

Catalysts	**Conditions**	**NH_3 yield rate**	**FE (%)**	**Ref.**
FeS_2/MoS_2 nanosheets	**0.1M Na_2SO_4**	**2.59 μmol·h^{-1}·mg^{-1} (44.03 μg·h^{-1}·mg^{-1} $_{cat.}$)**	**4.63%**	**This work**
MoS_2-rGO	0.1 M $LiClO_4$	24.82 μg·h^{-1}·mg$^{-1}_{cat.}$	4.58%	[8]
MoS_2-Fe	0.1 M Na_2SO_4	20.11 μg·h^{-1}·mg$^{-1}_{cat.}$	15.72%	[9]
VS-MoS_2	0.1 M Na_2SO_4	29.55 μg·h^{-1}·mg$_{cat.}^{-1}$	4.58 %	[10]
Fe-MoS_2	0.5 M K_2SO_4	8.63 μg·h^{-1}·mg$_{cat.}^{-1}$	18.8 %	[11]
$Fe_2(MoO_4)_3$	0.1 M Na_2SO_4	7.5 μg·h^{-1}·mg$_{cat.}^{-1}$	1.0 %	[12]
MoS_2 QDs	0.5 M $LiClO_4$	39.6 μg h^{-1} mg^{-1}	12.9%	[13]
MoS_2@$Fe(OH)_3$/CC	0.1 M Na_2SO_4	4.23 × 10^{-10} mol s^{-1} cm^{-2}	2.76%	[14]
FeS_2−MoS_2	0.1 M KOH	7.1×10^{-4} μmol·s^{-1}·cm^{-2}	4.6%	[15]
FeS@MoS_2/CFC	Na_2SO_4	8.45 μg·h^{-1}·cm^{-2}	2.96%	[16]
MoS_2-800	0.1 M HCl	23.38 μg·h^{-1}·mg$^{-1}_{cat.}$	17.9%	[17]

References

1. P. L. Searle, *The Analyst*, 1984, **109**, 549.
2. G. W. Watt and J. D. Chrisp, *Analytical Chemistry*, 1954, **26**, 452-453.
3. G. Kresse and J. Furthmüller, *Computational Materials Science*, 1996, **6**, 15-50.
4. G. Kresse and J. Furthmüller, *Physical Review B*, 1996, **54**, 11169-11186.
5. J. P. Perdew, K. Burke and M. Ernzerhof, *Physical review letters*, 1996, **77**, 3865-3868.
6. P. E. Blöchl, *Physical review. B, Condensed matter*, 1994, **50**, 17953-17979.
7. J.-Y. Zhao and J.-M. Zhang, *The Journal of Physical Chemistry C*, 2017, **121**, 19334-19340.
8. X. Li, X. Ren, X. Liu, J. Zhao, X. Sun, Y. Zhang, X. Kuang, T. Yan, Q. Wei and D. Wu, *Journal of Materials Chemistry A*, 2019, **7**, 2524-2528.
9. L. Niu, D. Wang, K. Xu, W. Hao, L. An, Z. Kang and Z. Sun, *Nano Research*, 2021, **14**, 4093-4099.
10. B. Liu, C. Ma, D. Liu and S. Yan, *ChemElectroChem*, 2021, **8**, 3030-3039.
11. H. Su, L. Chen, Y. Chen, R. Si, Y. Wu, X. Wu, Z. Geng, W. Zhang and J. Zeng, *Angew Chem Int Ed Engl*, 2020, **59**, 20411-20416.
12. C. Chen, Y. Liu and Y. Yao, *European Journal of Inorganic Chemistry*, 2020, **2020**, 3236-3241.
13. Y. Luo, P. Shen, X. Li, Y. Guo and K. Chu, *Chem Commun*, 2021, **57**, 9930-9933.
14. X. Xu, X. Liu, J. Zhao, D. Wu, Y. Du, T. Yan, N. Zhang, X. Ren and Q. Wei, *J Colloid Interface Sci*, 2022, **606**, 1374-1379.
15. M. Yang, Z. Jin, C. Wang, X. Cao, X. Wang, H. Ma, H. Pang, L. Tan and G. Yang, *ACS Appl Mater Interfaces*, 2021, **13**, 55040-55050.
16. Y. Guo, Z. Yao, B. J. J. Timmer, X. Sheng, L. Fan, Y. Li, F. Zhang and L. Sun, *Nano Energy*, 2019, **62**, 282-288.
17. M. You, S. Yi, X. Hou, Z. Wang, H. Ji, L. Zhang, Y. Wang, Z. Zhang and D. Chen, *J Colloid Interface Sci*, 2021, **599**, 849-856.